Calculations of scattered light from rigid polymers by Shifrin and Rayleigh-Debye approximations

Marilyn F. Bishop
Department of Physics, Virginia Commonwealth University, Richmond, Virginia 23284-2000

ABSTRACT We show that the commonly used Rayleigh-Debye method for calculating light scattering can lead to significant errors when used for describing scattering from dilute solutions of long rigid polymers, errors that can be overcome by use of the easily applied Shifrin approximation. In order to show the extent of the discrepancies between the two methods, we have performed calculations at normal incidence both for polarized and unpolarized incident light with the scattering intensity determined as a function of polarization angle and of scattering angle, assuming that the incident light is in a spectral region where the absorption of hemoglobin is small. When the Shifrin method is used, the calculated intensities using either polarized or unpolarized scattered light give information about the alignment of polymers, a feature that is lost in the Rayleigh-Debye approximation because the effect of the asymmetric shape of the scatterer on the incoming polarized electric field is ignored. Using sickle hemoglobin polymers as an example, we have calculated the intensity of light scattering using both approaches and found that, for totally aligned polymers within parallel planes, the difference can be as large as 25%, when the incident electric field is perpendicular to the polymers, for near forward or near backward scattering (0° or 180° scattering angle), but becomes zero as the scattering angle approaches 90°. For randomly oriented polymers within a plane, or for incident unpolarized light for either totally oriented or randomly oriented polymers, the difference between the two results for near forward or near backward scattering is ~15%.

I. INTRODUCTION

Fibrous proteins that can be described approximately as long rigid cylindrical polymers appear in many biological contexts, showing a large range of diameters and lengths and biological functions. Some of these are an integral part of the structure, such as intracellular cytoskeletal structural proteins, including actin (in microfilaments of 7–9 nm in diameter) (O'Brien and Dickens, 1983), tubulin (in microtubules of 25 nm in diameter)(Amos, 1982; Purich and Kristofferson, 1984; Mitchison and Kirschner, 1984*a, b*) and intermediate filaments (7–11 nm in diameter) (Steinert, 1981). Also in this category are myosin filaments (110–150 nm in diameter) (Craig and Knight, 1982), which work in association with actin in muscle and many microscopic forms of cell motion; collagen (10–500 nm in diameter)(Serafini-Fracassini, 1982; Traub and Piez, 1971), a fibrous proteins of connective tissue and a major component of the cornea (Maurice, 1957, 1962; Goldman and Benedek, 1967; Hart and Farrell, 1969; Cox et al., 1970; Benedek, 1971; McCally and Farrell, 1976; Farrell and McCally, 1976; Andreo and Farrell, 1982); crystallin (Delaye and Tardieu, 1983), an eye lens protein; and fibrin (Casassa, 1955; Hantgan and Hermans, 1979), a plasma protein. Others are destructive, leading to disorders and diseases. These include sickle hemoglobin (20 nm in diameter) (Dykes et al., 1979), which as the result of a mutation forms fibers that rigidify the red blood cell and lead to sickle cell disease; many types of viruses, especially tobacco mosaic virus (15 nm) (Oster et al., 1947); and amyloid (4–22 nm in diameter) (A. S. Cohen et al., 1982), the fibrous tissue of amyloidosis, a disorder widespread in the animal kingdom. In order to calculate light scattering from a dilute solution of fibers from any of these systems, it is necessary to know only the dimensions and dielectric function or index of refraction of the fibers.

Elastic light scattering and turbidity have been widely used as a probe of the formation of fibers in solution since they can give information about the quantity of material polymerized, and if used to study the evolution of a system over time, provide information about the kinetics of polymerization. For example, studies have been done with epidermal keratin intermediate filaments (Steinert et al., 1976), actin (Wegner, 1982; Wegner and Savko, 1982), microtubules (Gaskin et al., 1974, Berne, 1974), collagen in the cornea (Maurice, 1962; Hart and Farrell, 1969; Benedek, 1971; McCally and Farrell, 1976; Farrell and McCally, 1976; Andreo and Farrell, 1982); crystallin (Delaye and Tardieu, 1983), fibrin (Casassa, 1955; Hantgan and Hermans, 1979), tobacco mosaic virus (Oster et al., 1947), and sickle hemoglobin (Pumphrey and Steinhardt, 1976; Hofrichter et al., 1978; Elbaum et al., 1978;

0006-3495/89/11/911/15 $2.00

Adachi and Asakura, 1978, 1979, 1982, 1983; Ferrone et al., 1980; Christoph and Briehl, 1983; Madonia et al., 1983; Ferrone et al., 1985*a*; Hofrichter, 1986; Briehl and Christoph, 1987; Ferrone, et al., 1987; Basak et al., 1988). If the polymerized particles are nonspherical in shape, analysis of the angular distribution of scattering, the wavelength dependence, and the polarization of the scattered light can give information about the shape and alignment of polymers (van de Hulst, 1981; Bohren and Huffman, 1983; Camerini-Otero and Day, 1978; Berne, 1974).

This paper shows that the usual Rayleigh-Debye approximation (Zimm et al., 1945; Debye, 1947; Zimm, 1948; Debye and Bueche, 1950; Zimm and Dandliker, 1954; Landau and Lifshitz, 1960; Tanford, 1961; Kerker, 1969; Kratochvil, 1972; Berne, 1974; Berne and Pecora, 1976; van de Hulst, 1981; Bohren and Huffman, 1983; Burchard, 1983) for the analysis of polarized elastic light scattering from polymers can lead to significant errors, both qualitative and quantitative. The paper further shows that some of these can be overcome with the use of the equally simple Shifrin approximation (Shifrin, 1951), as modified by Acquista (1976, 1980) and L. D. Cohen et al. (1983), which yields the same result as the exact solution of Maxwell's equations (Mie theory) where that is available. We will assume here that the concentration of polymers in solution is sufficiently dilute that the polymers scatter independently, so that the total intensity of light scattering, i.e., the turbidity, is simply proportional to the concentration of monomers incorporated into polymers.

As a qualitative illustration of these theoretical limitations of the Rayleigh-Debye method, we will consider sickle hemoglobin, which polymerizes when deoxygenated into long rigid polymers. (Ferrone et al., 1980, 1985*b*, 1987; Hofrichter, 1986, Eaton and Hofrichter, 1987; Basak et al., 1988). In the early stages of polymerization of sickle hemoglobin, i.e., the first 10% of the reaction, the concentration of polymers is sufficiently low that the assumptions of this paper should apply, even if the polymers form clumps of aligned polymers such that the radii of clumps are much less than the wavelength of light. In addition, if the samples are prepared in a high phosphate solution, the concentration of polymers remains low throughout the time course of the reaction (Adachi and Asakura, 1978, 1979, 1982, 1983) and the approximations of this paper may apply to the entire time course of the reaction.

The paper is organized as follows. In Sec. II, we present the Rayleigh-Debye method for light scattering, and in Sec. III the Shifrin method. In Sec. IV, we derive the exact (Mie) solution for light scattering from a infinitely long cylinder and show that the Shifrin method, and not the Rayleigh-Debye method, agrees with this result to first order in small quantities. In Sec. V, we present results of calculations using the Shifrin and Rayleigh-Debye approaches for the case of sickle hemoglobin polymers in solution in order to illustrate the qualitative and quantitative differences in the results. In Sec. VI, we present the conclusions, and in the Appendix, we explain our method for determining the dielectric constant inside a sickle hemoglobin polymer and the effective dielectric constant for the hemoglobin solution surrounding the polymers.

II. RAYLEIGH-DEBYE METHOD

The Rayleigh-Debye, or Rayleigh Gans, method for calculating the light scattered from small particles is an extension of the Rayleigh scattering method for very small (spherical) particles. In Rayleigh scattering, one assumes that a light beam incident on a particle small compared with the wavelength λ induces an oscillating dipole in that particle, which in turn produces scattered radiation in the form of a spherical wave. For unpolarized incident light with intensity I_0, the scattered intensity is given by the well-known formula (Landau and Lifshitz, 1960; Tanford, 1961; Kerker, 1969; van de Hulst, 1981; Bohren and Huffman, 1983),

$$I = [I_0 k_0^4 |\alpha|^2 / 2r^2](1 + \cos^2\theta), \tag{2.1}$$

where α is the polarizability of the particle, $k_0 = 2\pi/\lambda$ is the wave vector of the incident light, r is the distance from the scattered particle to the observer, and θ is the angle of scattering relative to the incident beam. If the particle is assumed to be spherical with radius a, and if m_a, the index of refraction inside the particle divided by the index of refraction of the surrounding medium, is close to one, i.e., $m_a \approx 1$, then α is given by

$$\alpha = a^3(m_a^2 - 1)/(m_a^2 + 2) \approx (V/2\pi)(m_a - 1). \tag{2.2}$$

where $V = (4\pi/3)a^3$ is the volume of the particle. In order for the Rayleigh approximation to be valid, one must satisfy both the conditions that $a \ll \lambda/2\pi$ and that $|(m_a - 1)|a \ll \lambda/2\pi$, i.e., not only should the particle be small compared with the wavelength outside the particle, but also compared with the wavelength inside the particle.

In Rayleigh-Debye scattering (Zimm et al., 1945; Debye, 1947; Zimm, 1948; Debye and Bueche, 1950; Zimm and Dandliker, 1954; Landau and Lifshitz, 1960; Tanford, 1961; Kerker, 1969; Kratochvil, 1972; Berne, 1974; van de Hulst, 1981; Bohren and Huffman, 1983), larger particles are assumed to be composed of arrays of small spherical particles, each with a polarizability α as given in Eq. 2.2 above, with the approximation that the

index of refraction should not vary appreciably from that of the surroundings, i.e., $|(m_a - 1)| \ll 1$. However, the conditions stated above for Rayleigh scattering must now be satisfied by the largest dimension of the particle. Because of the simplicity of this method, the results are used in a wide range of applications, and unfortunately often beyond this domain of validity. In the following sections, we will discuss some of the consequences of this misuse.

In order to illustrate the Rayleigh-Debye method, we begin with the introduction of a coordinate system in which we allow a specific polarization for both the incident and scattered light beams (See Fig. 1). We assume that the direction of propagation of the incident beam of light, with wave vector $\mathbf{k}_0$, is along the unit vector $\mathbf{e}_z$ (in the positive z direction) and the direction of the scattered beam, with wave vector $\mathbf{k}_s$, is along the unit vector $\mathbf{e}_r$, where both wave vectors have the same magnitude $k_0 = 2\pi/\lambda$, and where $\mathbf{e}_r$ is in the direction $\mathbf{r}$ specified by the angles θ and ϕ. The scattering plane is then defined as the plane containing both $\mathbf{e}_z$ and $\mathbf{e}_r$. The directions of the incident electric field for parallel and perpendicular polarizations relative to the scattering plane are in the x-y plane and are given by the unit vectors $\mathbf{e}_{0\parallel}$ and $\mathbf{e}_{0\perp}$, where $\mathbf{e}_{0\perp} \times \mathbf{e}_{0\parallel} = \mathbf{e}_z$, the direction of propagation of the incident beam. In order for the cross product of the scattered field directions to be in the direction $\mathbf{e}_r$ of the scattered beam, we choose $\mathbf{e}_{s\parallel} = \mathbf{e}_\theta$ and $\mathbf{e}_{s\perp} = \mathbf{e}_{0\perp} = -\mathbf{e}_\phi$, so that $\mathbf{e}_{s\perp} \times \mathbf{e}_{s\parallel} = \mathbf{e}_r$.

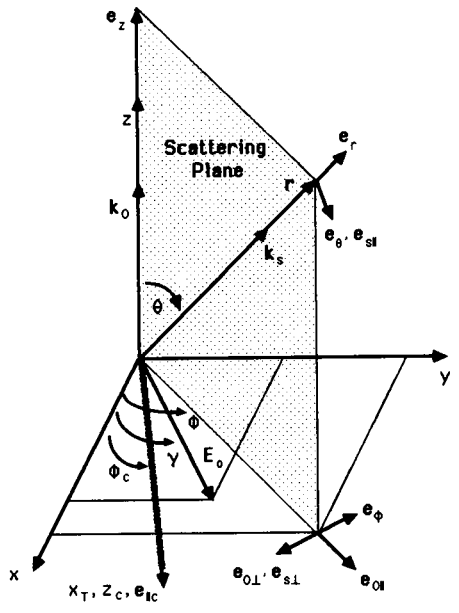

FIGURE 1 Geometry for light scattering calculations, where $\mathbf{k}_0$ is in the direction of the incident beam and $\mathbf{k}_s$ is in the direction of the detector. The polymer from which the light is scattered has its axis in the x-y plane along the direction x_T, z_c, or $\mathbf{e}_{lc}$, as shown. The scattering plane is defined by the vectors $\mathbf{k}_0$ and $\mathbf{k}_s$. Other variables are defined in the text.

Suppose the polarization of the incident beam is such that the incident electric field $\mathbf{E}_0$ makes an angle γ with the x-axis in Fig. 1. Then in terms of these unit vectors,

$$\begin{aligned}\mathbf{E}_0 &= e^{i(k_0 z - \omega t)}\,[E_{0\parallel}\mathbf{e}_{0\parallel} + E_{0\perp}\mathbf{e}_{0\perp}] \\ &= E_0 e^{i(k_0 z - \omega t)}\,[\cos(\phi - \gamma)\mathbf{e}_{0\parallel} + \sin(\phi - \gamma)\mathbf{e}_{0\perp}],\end{aligned} \tag{2.3}$$

so that if $(\phi - \gamma) = 0$, then the incident field $\mathbf{E}_0$ is parallel to the scattering plane, and if $(\phi - \gamma) = \pi/2$, it is perpendicular to that plane. If we then write the scattered electric field as

$$\mathbf{E}_s = [E_{s\parallel}\mathbf{e}_{s\parallel} + E_{s\perp}\mathbf{e}_{s\perp}], \tag{2.4}$$

then the incident and scattered fields are related by

$$\begin{pmatrix} E_{s\parallel} \\ E_{s\perp} \end{pmatrix} = \left(\frac{k_0^2(m_a - 1)}{2\pi r}\right) e^{i(k_0 r - \omega t)}\, V f(\theta, \phi) \begin{pmatrix} E_{0\parallel}\cos\theta \\ E_{0\perp} \end{pmatrix}, \tag{2.5}$$

where V is the total volume of the sample and $f(\theta, \phi)$ is the scattering form factor. If $f(\theta, \phi)$ were equal to one, then these expressions would be precisely what one obtains for Rayleigh scattering. This form factor is a sum over all the phases δ of different parts of the particle relative to an arbitrary origin and, if we assume that all parts of the particle have the same polarizability, may be written in integral form as

$$f(\theta, \phi) = (1/V)\int_V e^{i\delta}\, dV. \tag{2.6a}$$

The relative phase δ of various points in the body is given by

$$\delta = k_0 \mathbf{R} \cdot (\mathbf{e}_z - \mathbf{e}_r), \tag{2.6b}$$

where $\mathbf{R}$ is the vector from the origin to the point of scattering. In these expressions, we assume that the particle is much smaller than the distance to the point of observation. The factor $\cos\theta$ in Eq. 2.5 for $E_{s\parallel}$ is a purely geometrical factor. For the incident field parallel to the scattering plane, factor $\cos\theta$ projects the incident field into a plane perpendicular to the scattered wave vector $\mathbf{k}_s$, while for the incident field perpendicular to the scattering plane, the factor is unity, since the incident field is already perpendicular to $\mathbf{k}_s$.

Once we know the scattered field, the complex Poynting vector $\mathbf{S}$ is given by

$$\mathbf{S} = (c/8\pi)\mathbf{E} \times \mathbf{H}^*, \tag{2.7}$$

where the real part is the time averaged intensity of light in the direction of propagation of the beam. If r is sufficiently large that we are in the far field region, we have for the scattered Poynting vector:

$$\mathbf{S}_s = (ck_0/8\pi\omega)\,|\mathbf{E}_s|^2\mathbf{e}_r = I_0|\mathbf{E}_s|^2/|\mathbf{E}_0|^2\mathbf{e}_r = I\mathbf{e}_r, \tag{2.8}$$

where I and I_0 are the intensities of the incident and scattered light, respectively. Thus from Eqs. 2.5, 2.7, and 2.8, we find that, for specific incident polarizations either parallel or perpendicular to the scattering plane, the scattered Poynting vector is:

$$\begin{pmatrix} \mathbf{S}_{s\parallel} \\ \mathbf{S}_{s\perp} \end{pmatrix} = \left[\frac{k_0^4(m_a - 1)^4}{(2\pi r)^2}\right] I_0 V^2 f^2(\theta, \phi) \begin{bmatrix} (E_{0\parallel}^2/E_0^2)\cos^2\theta \\ (E_{0\perp}^2/E_0^2) \end{bmatrix} \tag{2.9}$$

Alternatively, the scattered field may be written in terms of a unit polarization vector $\mathbf{e}_{ps,RD}$ in the direction of the scattered field. In terms of unit vectors parallel and perpendicular to the plane of scattering, where we write the incident field as in Eq. 2.3, this unit polarization vector may be written as

$$\mathbf{e}_{ps,RD} = [\cos\theta\cos(\phi - \gamma)\mathbf{e}_{s\parallel} + \sin(\phi - \gamma)\mathbf{e}_{s\perp}]/T_{p,RD}, \tag{2.10a}$$

where

$$T_{p,RD} = [\cos^2\theta\cos^2(\phi - \gamma) + \sin^2(\phi - \gamma)]^{1/2}. \tag{2.10b}$$

The unit vector perpendicular both to $\mathbf{k}_s$ and to $\mathbf{e}_{ps,RD}$ is then given by:

$$\mathbf{e}_{ps,\perp RD} = [-\sin(\phi - \gamma)\mathbf{e}_{s\parallel} + \cos\theta\cos(\phi - \gamma)\mathbf{e}_{s\perp}]/T_{p,RD}. \tag{2.10c}$$

This will be used later in Sec. V in the comparison of results of the Shifrin method with those of the Rayleigh-Debye method.

Using Eq. 2.10, the scattered field may be written, as an alternative to Eq. 2.5, in the simplified form

$$\mathbf{E}_s = [k_0^2(m_a - 1)/2\pi r]E_0 e^{i(k_0 r - \omega t)} V f(\theta, \phi) T_p \mathbf{e}_{ps,RD}. \tag{2.11}$$

Note that when $\theta = 0$ (forward scattering), the scattered field is parallel to the incident field. This will not necessarily be true in the Shifrin method, as we will see.

For scattering from a circular cylinder, the angular scattering form factor $f(\theta, \phi)$ may be obtained by the following procedure. First perform the integration given by Eq. 2.6a over a representative circular disk of radius a, with y extending from the center of the disk to the radius, and second, sum all the disks along the length of the cylinder, with z ranging from $-\ell/2$ to $\ell/2$. The total expression then becomes

$$f(\theta, \phi) = F[2k_0 a \sin(\theta/2)\sin\psi] \cdot G[k_0\ell\sin(\theta/2)\cos\psi], \tag{2.12}$$

with

$$F(u) = 2J_1(u)/u; \qquad G(u) = \sin u/u, \tag{2.13}$$

where $J_1(u)$ is the Bessel function of the first kind of order one. In this expression, ψ is defined in terms of the angle ζ between the cylinder axis (or the axis of a single disk) and the incident beam and in terms of the angles θ and ϕ of Fig. 1 that determine the direction of propagation of the scattered beam:

$$\cos\psi = -\cos\zeta\sin(\theta/2) + \sin\zeta\cos(\theta/2)\cos(\phi - \phi_c), \tag{2.14}$$

where ϕ_c is the angle of the cylinder axis relative to the x-axis.

For a thin rod, i.e., $k_0 a \ll 1$, $f(\theta,\phi)$ reduces to

$$f_{thin}(\theta,\phi) = G[(k_0\ell\sin(\theta/2)\cos\psi]. \tag{2.15}$$

For light incident perpendicular to the cylinder axis, $\zeta = 90^0$ and $\cos\psi = \cos(\theta/2)\cos(\phi - \phi_c)$, so that

$$f_\perp(\theta, \phi) = F\{k_0 a[2(1 - \cos\theta) - \sin^2\theta\cos^2(\phi - \phi_c)]^{1/2}\} \cdot G\{(k_0\ell/2)\sin\theta\cos(\phi - \phi_c)\}. \tag{2.16}$$

For a thin rod, i.e., $k_0 a \ll 1$, Eq. 2.16 reduces to

$$f_{\perp,thin}(\theta, \phi) = G\{(k_0\ell/2)\sin\theta\cos(\phi - \phi_c)\}. \tag{2.17}$$

For a long thin rod, $f_{\perp,thin}(\theta,\phi)$ peaks sharply at $(\phi - \phi_c) \approx 90^0$, and is essentially zero away from this value, so the cos $(\phi - \phi_c) \approx 0$. This means that θ can take any value from 0 to π without affecting the position of this scattering peak. The physical consequence of this is that light is scattered mostly in directions perpendicular to the cylinder axis.

In order to compare the angular dependence of Rayleigh-Debye scattering for a cylinder with Rayleigh scattering from a sphere, it is useful to write the ratio of the scattered to incident intensities for Rayleigh-Debye scattering, which comes simply from combining Eqs. 2.8 and 2.11:

$$\begin{aligned} I/I_0 &= (E_{s\parallel}^2 + E_{\perp s}^2)/E_0^2 \\ &= [k_0^4(m_a - 1)^2/(2\pi r)^2]V^2 f^2(\theta, \phi) \\ &\quad \cdot [\cos^2\theta\cos^2(\phi - \gamma) + \sin^2(\phi - \gamma)]. \end{aligned} \tag{2.18}$$

For unpolarized (natural) incident light, one must average over all angles γ, yielding the result:

$$I/I_0 = (1/2)[k_0^4(m_a - 1)^2/(2\pi r)^2]V^2 f^2(\theta,\phi)(\cos^2\theta + 1). \tag{2.19}$$

This is the same as averaging over values of ϕ, or averaging over all directions of cylinders within a plane perpendicular to the incident beam. From Eq. 2.19, it is clear that for Rayleigh-Debye scattering, the difference between cylinders and spheres lies completely in the factor $f^2(\theta, \phi)$, as can be seen by comparing with Eqs. 2.1 and 2.19, i.e., when $f^2(\theta, \phi) = 1$, Eq. 2.19 is identical with

Eq. 2.1. For particles oriented randomly, this factor must be averaged over all solid angles, giving the factor $P(\theta)$ by which the intensity of the Rayleigh formula has to be multiplied in order to obtain Rayleigh-Debye scattering:

$$P(\theta) = \overline{f^2(\theta, \phi)} = (1/4\pi) \int f^2(\theta, \phi)\, d\Omega, \qquad (2.20)$$

where the values of θ and ϕ are fixed and the integration over the solid angles ($d\Omega$) represents an average over all the orientations that the particles can have. For thin rods, using Eq. 2.15, this becomes

$$P(\theta) = \overline{f^2_{thin}(\theta, \phi)} = \int_0^1 G^2(z \cos \psi)\, d(\cos \psi)$$
$$= (1/z) \int_0^{2z} [\sin w/w]\, dw - [\sin z/z]^2, \qquad (2.21)$$

where $z = k_0 \ell \sin \theta/2$.

This same result, with randomly oriented cylinders and unpolarized incident light, has been obtained by other methods (Zimm et al., 1945; Debye, 1947; Zimm, 1948; Debye and Bueche, 1950; Zimm and Dandliker, 1954; Landau and Lifshitz, 1960; Tanford, 1961; Kerker, 1969; Kratochvil, 1972; Berne, 1974; Berne and Pecora, 1976; van de Hulst, 1981; Bohren and Huffman, 1983). In these derivations one usually obtains first an expression for $P(\theta)$ for any set of randomly oriented particles, given by

$$P(\theta) = (1/n^2) \sum_{i=1}^{n} \sum_{j=1}^{n} [\sin (\mu h_{ij})/\mu h_{ij}], \qquad (2.22)$$

where n is the number of scattering subunits, h_{ij} is the distance between the ith and jth subunits, and $\mu = (4\pi/\lambda) \sin (\theta/2)$. We will not use this approach, since we are interested in determining whether the polymers align, where the use of polarized incident and polarization analyzed scattered light is important.

III. SHIFRIN METHOD

One of the limitations of the Rayleigh-Debye method is the restriction on the dimensions of a particle, all of which must be smaller than the wavelength of light. Another method, originally introduced by Shifrin (1951) and more recently extended by Acquista (1976, 1980*a*) and L. D. Cohen et al. (1983) employs a method that is almost as simple to apply in practice, but that is free of this fundamental size limitation. The general method developed by Shifrin (1951) starts with Maxwell's equations for nonmagnetic particles, with no free charges or currents, assuming a harmonic time dependence $e^{-i\omega t}$, as in Sec. II, for the fields. Only two of Maxwell's equations, given by

$$\nabla \times \mathbf{E} = (i\omega/c)\mathbf{H}; \qquad \nabla \times \mathbf{H} = -(i\omega/c)\mathbf{D}, \qquad (3.1)$$

are necessary for this derivation. In order to solve these equations for a solution of particles, we define the Hertz vector $\mathbf{Z}$ such that

$$\mathbf{E} = \nabla(\nabla \cdot \mathbf{Z}) + k_0^2 \mathbf{Z}; \qquad H = -(ic/\omega)k_0^2(\nabla \times \mathbf{Z}); \qquad (3.2)$$

where $\mathbf{k}_0$ is the wave vector of the incident light, as in Sec. II, with $k_0^2 = (\omega^2/c^2)\epsilon_s$, where $\epsilon_s = n_s^2$ is the dielectric constant of the solution surrounding the particles of interest, with n_s the corresponding index of refraction. Eqs. 3.1 and 3.2 can be combined, using the vector identity, $\nabla \times \nabla \times \mathbf{Z} = \nabla(\nabla \cdot \mathbf{Z}) - \nabla^2 \mathbf{Z}$, to yield the simple form

$$\nabla^2 \mathbf{Z} + k_0^2 \mathbf{Z} = [\mathbf{E} - (1/\epsilon_s)\mathbf{D}] = [1 - (\epsilon/\epsilon_s)]\mathbf{E}, \qquad (3.3)$$

where the displacement vector is written as $\mathbf{D} = \epsilon \mathbf{E}$, with ϵ given by

$$\epsilon = \begin{cases} \epsilon_p & \text{inside the particles} \\ \epsilon_s & \text{in the solution surrounding the particles.} \end{cases} \qquad (3.4)$$

Eq. 3.3 may be solved by the Green's function method, yielding the following integral form for the Hertz vector:

$$\mathbf{Z} = [\mathbf{E}_0(\mathbf{r}) \cdot \mathbf{r}][\mathbf{k}_0/(ik_0^2)] \exp(i\mathbf{k}_0\mathbf{r}) - (1/4\pi) \int d^3r'$$
$$\cdot [1 - (\epsilon/\epsilon_s)]\mathbf{E}(\mathbf{r}') \exp[ik_0|\mathbf{r} - \mathbf{r}'|]/|\mathbf{r} - \mathbf{r}'|, \qquad (3.5)$$

where $\mathbf{r}$ is the vector from an arbitrary origin to the point of observation, $\mathbf{r}'$ is the vector from the origin to a point within the source of scattering, and $|\mathbf{r} - \mathbf{r}'|$ is the distance between the observational point and the point at which a source is located. The first term of this solution arises from the plane wave incident on the particle, and the second term from the response of the particles to this wave. Note that this second term contributes only for positions inside the particles, where $\epsilon = \epsilon_p$, since it is zero in the solution around the polymers, where $\epsilon = \epsilon_s$. Using Eq. 3.5, we may now write $\mathbf{E}(\mathbf{r})$ using its definition in terms of $\mathbf{Z}$, as given in Eq. 3.2, as:

$$\mathbf{E}(\mathbf{r}) = \mathbf{E}_0 \exp[i(\mathbf{k}_0 \cdot \mathbf{r} - \omega t)] + (1/4\pi)(\text{grad div} + k_0^2)$$
$$\cdot \int d^3r'[(\epsilon/\epsilon_s) - 1]\mathbf{E}(\mathbf{r}') \exp[ik_0|\mathbf{r} - \mathbf{r}'|]/|\mathbf{r} - \mathbf{r}'|. \qquad (3.6)$$

The first term on the right hand side of Eq. 3.6 is the incident electric field, and the second is the electric field caused by the scattering particle. The solution of Eq. 3.6 can be found by iteration as follows. One first proposes an approximate value for $\mathbf{E}(\mathbf{r}')$ on the right hand side of the equation and solves for $\mathbf{E}(\mathbf{r})$ on the left hand side. This new value of $\mathbf{E}(\mathbf{r})$ is now substituted as $\mathbf{E}(\mathbf{r}')$ on the right hand side and the process is repeated until the expression substituted in the right hand side agrees, to within the desired accuracy, with the value generated for the left hand side. The Shifrin approach is to estimate the electric field $\mathbf{E}(\mathbf{r})$ inside the particle from which the light is scattered, in terms of its static polarizability, and use this as the start of an iterative approach. The total field is then

written as a series of successive approximations to be determined by iteration, where the factor $[(\epsilon/\epsilon_s) - 1]/(4\pi)$ becomes the expansion parameter. To second order, $\mathbf{E}(\mathbf{r}) = \mathbf{E}_1(\mathbf{r}) + \mathbf{E}_2(\mathbf{r})$ becomes (Acquista, 1976; L. D. Cohen, et al., 1983):

$$\mathbf{E}(\mathbf{r}) \sim \mathbf{E}_0 \exp[i(\mathbf{k}_0 \cdot \mathbf{r} - \omega t)] + \{[(\epsilon/\epsilon_s) - 1]/(4\pi)\}\mathbf{E}_1 + \{[(\epsilon/\epsilon_s) - 1]/(4\pi)\}^2\mathbf{E}_2. \quad (3.7)$$

Here, the term containing $\mathbf{E}_1(\mathbf{r})$ is the first order approximation to the solution and the term containing $\mathbf{E}_2(\mathbf{r})$ is the second order approximation.

Alternatively, the simplest solution of the integral equation would be to substitute the zeroth order electric field (i.e., the incident electric field) into the integral and iterate. The first approximation in this scheme is actually the Rayleigh-Debye result (Acquista, 1976), as we will show later. For a long cylinder, the convergence of such a scheme is slow, while for the Shifrin approach, which employs the internal solution for an infinite dielectric cylinder in a uniform electrostatic field, the convergence is improved considerably for long cylinders. In fact, L. D. Cohen, et al. (1983) have shown that convergence is greatly enhanced for cylinders with an aspect ratio (length to diameter ratio) of 20 or greater, with the first order approximation yielding an accuracy of better than 1%, for $(\epsilon/\epsilon_s) = 1.5$. [In the case of HbS polymers, $(\epsilon/\epsilon_s) = 1.27$, as shown in the Appendix, which should allow the same accuracy with much smaller aspect ratios.]

The static polarizability for an infinitely long dielectric cylinder was used in this approximate scheme to obtain $E_1(\mathbf{r})$, the jth component of the total electric field in terms of $E_{\text{eff}j}(\mathbf{r})$, the components of the effective polarizing field inside the cylinder. Using the Cartesian coordinates in the cylinder coordinate system, this relation is:

$$E_i(\mathbf{r}) = \sum_j A_{ij} E_{\text{eff}\,j}(\mathbf{r}), \quad (3.8a)$$

where

$$\mathbf{A} = \begin{pmatrix} A_{\perp c} & 0 & 0 \\ 0 & A_{\perp c} & 0 \\ 0 & 0 & A_{\parallel c} \end{pmatrix}. \quad (3.8b)$$

Here $\alpha_{\perp c} = \{[(\epsilon/\epsilon_s) - 1]/(4\pi)\}A_{\perp c}$ is the polarizability with the electric field perpendicular to the axis of the cylinder, and $\alpha_{\parallel c} = \{[(\epsilon/\epsilon_s) - 1]/(4\pi)\}A_{\parallel c}$ is the polarizability with the electric field parallel to the axis of the cylinder. The first order solution is found from Eq. 3.7 by keeping all terms up to and including $\{[(\epsilon/\epsilon_s) - 1]/(4\pi)\}\mathbf{E}_1$, where the ith component of $\mathbf{E}_1$ is given by (Acquista, 1976):

$$E_{1i} = \int d^3r' \sum_j (\partial^2/\partial x_i \partial x_j + k_0^2\delta_{ij}] \sum_m A_{jm} E_{0m}(\mathbf{r}') \cdot U(\mathbf{r}') \exp(i\mathbf{k}_0 \cdot \mathbf{r}') \exp[ik_0|\mathbf{r} - \mathbf{r}'|]/|\mathbf{r} - \mathbf{r}'|, \quad (3.9a)$$

$$U(\mathbf{r}) = \begin{cases} 1, & \text{inside the particle} \\ 0, & \text{outside the particle.} \end{cases} \quad (3.9b)$$

In this order the effective field inside the cylinder is taken to be the incident field i.e., $\mathbf{E}_{\text{eff}}(\mathbf{r}') = \mathbf{E}_0(\mathbf{r}')$. We have written (grad div + k_0^2) explicitly in terms of Cartesian components, where $E_{0m}(\mathbf{r}')$ is the mth Cartesian component of $\mathbf{E}_0(\mathbf{r}')$. If $A_{\perp c} = A_{\parallel c}$, then in first order one would recover the Rayleigh-Debye theory. The expression may be simplified for the case of a cylindrical particle as (L. D. Cohen et al., 1983):

$$\mathbf{E}_1 = \{\exp[i(k_0 r - \omega t)]/r\} k_0^2 u(k_0^2 \mathbf{e}_r - \mathbf{k}_0) \cdot E_0 A_{\parallel c}\, T_{p,\text{Shifrin}} \mathbf{e}_{ps,\text{Shifrin}} \quad (3.10a)$$

where

$$E_0 A_{\parallel c} T_{p,\text{Shifrin}}\, \mathbf{e}_{ps,\text{Shifrin}} = [(E_{0xc}\mathbf{e}_{xc} + E_{0yc}\mathbf{e}_{yc})A_{\perp c} + E_{0zc}\mathbf{e}_{zc}A_{\parallel c}]_\perp, \quad (3.10b)$$

where $\mathbf{e}_r$ is a unit vector in the direction of the scattered light entering the detector, $\mathbf{k}_0$ is the wave vector of the incident wave, and $[]_\perp$ means that the component of the enclosed vector that is perpendicular to the detector direction $\mathbf{e}_r$ should be taken. The pupil function $u(\mathbf{K})$ is the Fourier transform of $U(\mathbf{r})$ and is written for a cylinder as

$$u(\mathbf{K}) = \int d^3r'\, U(\mathbf{r}') \exp(i\mathbf{K} \cdot \mathbf{r}') = \pi a^2 \ell F(K_{\perp c} a) G(K_{\parallel c}\ell/2). \quad (3.11)$$

$F(u)$ and $G(u)$ are the functions defined in Eq. 2.13. In these functions, $\mathbf{K} = (k_0\mathbf{e}_r - \mathbf{k}_0)$, where $K_{\parallel c}$ and $K_{\perp c}$ are the components of $\mathbf{K}$ parallel and perpendicular to the cylinder axis, given for light incident perpendicular to the axis of the cylinder by

$$K_{\parallel c} = k_0 \sin\theta \cos(\phi - \phi_c) \quad (3.12a)$$

$$K_{\perp c} = k_0[2(1 - \cos\theta) - \cos^2\theta \sin^2(\phi - \phi_c)]^{1/2}. \quad (3.12b)$$

This means that $u(\mathbf{K})$ may be written simply as

$$u(\mathbf{K}) = Vf(\theta, \phi), \quad (3.13)$$

where V is the volume of the cylinder, and where $f(\theta,\phi)$ is given by Eq. 2.12 for a general cylinder or by Eq. 2.15 for a thin cylinder. For a long, thin rod, the factor $f(\theta,\phi)$ again restricts scattering to the plane perpendicular to the axis of the cylinder, as in Sec. II for Rayleigh-Debye scattering, so that only rods for which $\phi_c \approx \phi - \pi/2$

contribute to the scattering intensity in that direction. The total scattered field in the first order approximation may thus be written as

$$\mathbf{E}_s = k_0^2\{(m_a^2 - 1)/(4\pi r)\} \cdot [\exp[i(k_0 r - \omega t)]Vf(\theta, \phi)E_0 T_{p,\text{Shifrin}}\mathbf{e}_{ps,\text{Shifrin}}, \quad (3.14)$$

where the polarization factor $T_{p,\text{Shifrin}}\mathbf{e}_{ps,\text{Shifrin}}$ given in Eq. 3.10, for a long thin cylinder now becomes

$$\mathbf{e}_{ps,\text{Shifrin}} = \{[\cos\theta\cos(\phi - \gamma)(A_{\perp c}/A_{\parallel c})]\mathbf{e}_{s\parallel} + \sin(\phi - \gamma)\,\mathbf{e}_{s\perp}\}/T_{p,\text{Shifrin}} \quad (3.15a)$$

and

$$T_{p,\text{Shifrin}} = \{\cos^2\theta\cos^2(\phi - \gamma)(A_{\perp c}/A_{\parallel c})^2 + \sin^2(\phi - \gamma)\}^{1/2}. \quad (3.15b)$$

Note that the scattered field is not, in general, in the direction of the incident field for $\theta = 0$, as it was for Rayleigh-Debye scattering (see Eqs. 2.3 and 2.10). However, when $A_{\perp c} = A_{\parallel c}$, $\mathbf{e}_{ps,\text{Shifrin}}$ given by Eq. 3.15 reduces to the polarization direction $\mathbf{e}_{ps,RD}$ as in Eq. 2.10 for Rayleigh-Debye scattering. The polarization factors $A_{\perp c}$ and $A_{\parallel c}$, in the limit of a long thin rod, assume the simple form:

$$A_{\perp c} = 2/(m_a^2 + 1); \qquad A_{\parallel c} = 1. \quad (3.16)$$

For initial polarizations either completely parallel to the scattering plane ($\gamma - \phi = 0$) or completely perpendicular to that plane ($\gamma - \phi = \pi/2$), the scattered Poynting vector becomes:

$$\begin{pmatrix} \mathbf{S}_{s\parallel} \\ \mathbf{S}_{s\perp} \end{pmatrix} = \left(\frac{k_0^4(m_a^2 - 1)^2}{(4\pi r)^2}\right) \cdot I_0 V^2 f^2(\theta, \phi) \begin{bmatrix} (E_{0\parallel}^2/E_0^2)\cos^2\theta\,(A_{\perp c}/A_{\parallel c})^2 \\ (E_{0\perp}^2/E_0^2) \end{bmatrix} \mathbf{e}_r \quad (3.17)$$

where the factor $f^2(\theta, \phi)$ contains the restriction that only cylinders whose axes are perpendicular to the scattering plane can contribute to the scattering intensity.

If we assume that the polymers are all long compared with the wavelength of light, then $\phi \approx \phi_c$ and the polarization of the electric field reduces to

$$\mathbf{e}_{ps,\text{Shifrin}} = \{(A_{\perp c}/A_{\parallel c})\cos\theta\cos(\phi - \gamma)\mathbf{e}_{s\parallel} + \sin(\phi - \gamma)\mathbf{e}_{s\perp}\}/T_{p,\text{Shifrin}} \quad (3.18a)$$

and

$$T_{p,\text{Shifrin}} = \{(A_{\perp c}/A_{\parallel c})^2\cos^2\theta\cos^2(\phi - \gamma) + \sin^2(\phi - \gamma)\}^{1/2}. \quad (3.18b)$$

The normalized intensity for an arbitrary polarization of the incident light, as in Eq. 2.18 may thus be written from Eqs. 2.8, 3.14, and 3.15 as

$$(I/I_0)_{\text{Shifrin}} = (E_{\parallel s}^2 + E_{\perp s}^2)/E_0^2 = [k_0^4(m_a^2 - 1)^2/(4\pi r)^2]V^2 f^2(\theta, \phi) \cdot (\cos^2\theta\cos^2(\phi - \gamma)(A_{\perp c}/A_{\parallel c})^2 + \sin^2(\phi - \gamma)\}. \quad (3.19)$$

This may be decomposed into components parallel (polarized component) and perpendicular (rotated component) to the polarization of Rayleigh-Debye scattering, using Eq. 2.10 and 3.18. The polarized component is given by

$$(\mathbf{e}_{ps,\text{Shifrin}})_{RD-Pol} = (\mathbf{e}_{ps,\text{Shifrin}} \cdot \mathbf{e}_{ps,RD})\mathbf{e}_{ps,RD} = \{(A_{\perp c}/A_{\parallel c})\cos^2\theta\cos^2(\phi - \gamma) + \sin^2(\phi - \gamma)\}\mathbf{e}_{ps,RD}/(T_{p,\text{Shifrin}}\,T_{p,RD}) \quad (3.20)$$

and the rotated component is given by

$$(\mathbf{e}_{ps,\text{Shifrin}})_{RD-Rot} = (\mathbf{e}_{ps,\text{Shifrin}} \cdot \mathbf{e}_{ps,\perp RD})\mathbf{e}_{ps,\perp RD} = \{\cos\theta\cos(\phi - \gamma)\sin(\phi - \gamma) \cdot [1 - (A_{\perp c}/A_{\parallel c})]\}\mathbf{e}_{ps,\perp RD}/(T_{p,\text{Shifrin}}\,T_{p,RD}). \quad (3.21)$$

The normalized intensity for the polarized component is then given by

$$(I/I_0)_{\text{Shifrin},RD-Pol} = [k_0^4(m_a^2 - 1)^2/(4\pi r)^2]V^2 f^2(\theta, \phi) \cdot \{(A_{\perp c}/A_{\parallel c})\cos^2\theta\cos^2(\phi - \gamma) + \sin^2(\phi - \gamma)\}^2/(T_{p,RD})^2 \quad (3.22)$$

and for the rotated component is given by:

$$(I/I_0)_{\text{Shifrin},RD-Rot} = [k_0^4(m_a^2 - 1)^2/(4\pi r)^2]V^2 f^2(\theta, \phi) \cdot \{\cos\theta\cos(\phi - \gamma)\sin(\phi - \gamma) \cdot [1 - (A_{\perp c}/A_{\parallel c})]\}^2/(T_{p,RD})^2. \quad (3.23)$$

For unpolarized (natural) incident light, or for randomly oriented polymers within a plane, one must average over all angles γ, yielding the results:

$$(I/I_0)_{\text{Shifrin,unpol}} = (1/2)[k_0^4(m_a^2 - 1)^2/(4\pi r)^2] \cdot V^2 f^2(\theta, \phi)\{(A_{\perp c}/A_{\parallel c})^2\cos^2\theta + 1\} \quad (3.24a)$$

$$(I/I_0)_{\text{Shifrin},RD-Pol,unpol} = (1/2)[k_0^4(m_a^2 - 1)^2/(4\pi r)^2]V^2 f^2(\theta, \phi) \cdot \{(A_{\perp c}/A_{\parallel c})\cos^2\theta + 1\}^2/(T_{p,RD})^2; \quad (3.24b)$$

$$(I/I_0)_{\text{Shifrin},RD-Rot,unpol} = (1/8)[k_0^4(m_a^2 - 1)^2/(4\pi r)^2]V^2 f^2(\theta, \phi) \cdot \{\cos\theta[1 - (A_{\perp c}/A_{\parallel c})]\}^2/(T_{p,RD})^2. \quad (3.24c)$$

In order to compare with Rayleigh-Debye scattering, we make the approximation $m_a \approx 1$, and then Eqs. 3.19 and 3.24 reduce to the same results as in the Rayleigh-Debye method, as given in Eqs. 2.18 and 2.19. Thus, the main difference between the Rayleigh-Debye and Shifrin results is in the direction of polarization of the scattered light, for linearly polarized incident light, when m_a is not

very close to unity. The deviations of the relative index of refraction from unity for sickle hemoglobin polymers are, in fact, sufficiently large to produce large measurable effects, as we will see in Sec. V.

IV. MIE SCATTERING APPROACH FOR AN INFINITE CYLINDER

For an infinitely long cylindrical particle, an infinite series expansion solution can be found by solving Maxwell's equations and corresponding boundary conditions by using the same approach as for Mie scattering from a sphere (van de Hulst, 1981; Bohren and Huffman, 1983). The approach begins with Maxwell's Equations, i.e., Eq. 3.1, combined with $\nabla \cdot \mathbf{E} = 0$ and $\nabla \cdot \mathbf{H} = 0$, assuming that dielectric functions both inside and outside the particle are isotropic. Then both **E** and **H** satisfy vector wave equations of the form

$$\nabla^2\mathbf{E} + k^2\mathbf{E} = 0, \qquad \nabla^2\mathbf{H} + k^2\mathbf{H} = 0, \tag{4.1}$$

where **k** is the local propagation vector, with $k^2 = \epsilon\omega^2/c^2$, and ϵ is the dielectric constant either inside or outside the particle, as given in Eq. 3.4. Two new vector functions **M** and **N** are introduced, and these are defined in terms of a scalar function ψ and an arbitrary constant vector **c** by the forms

$$\mathbf{M} = \nabla \times (\mathbf{c}\psi), \qquad \mathbf{N} = (\nabla \times \mathbf{M})/k, \tag{4.2}$$

so that $\nabla \times \mathbf{N} = k\mathbf{M}$. Then one finds that

$$\nabla^2\mathbf{M} + k^2\mathbf{M} = \nabla \times [\mathbf{c}(\nabla^2\psi + k^2\psi)], \tag{4.3}$$

so that if the scalar function ψ satisfies the scalar wave equation $(\nabla^2\psi + k^2\psi = 0)$, then **M** satisfies the same vector wave equation as do the electric and magnetic fields in Eq. 4.1. When written in cylindrical coordinates (ρ, θ_c, z_c), with the z_c-axis along the length of the cylinder as in Fig. 1, the solutions are of the form

$$\psi_n(\rho, \theta_c, z_c) = Z_n(\rho)\, e^{in\theta_c} e^{ihz_c} \qquad (n = 0, \pm 1, \ldots), \tag{4.4}$$

where the $Z_n(\rho)$ are Bessel functions of the first and second kind, $J_n(\rho)$ and $Y_n(\rho)$, of integral order n. Vector cylindrical harmonics **M** and **N** are next generated in terms of these functions by combining Eqs. 4.2 and 4.4. The electric and magnetic fields, both incident and scattered, are then written as expansions in terms of these vector cylindrical harmonics. The usual Maxwell boundary conditions are employed to determine the unknown coefficients in these expansions. Finally, for large distances from the cylinder, $kr \gg 1$, the asymptotic forms of the fields are found.

For normal incidence on the cylinder, the scattered fields polarized parallel and perpendicular to the cylinder axes are given by

$$\begin{pmatrix} E_{s\parallel c} \\ E_{s\perp c} \end{pmatrix} = \left(\frac{2e^{3\pi i/4}}{(2\pi k_0\rho)^{1/2}}\right) e^{i(k_0\rho - \omega t)} \begin{pmatrix} T_1 E_{0\parallel c} \\ T_2 E_{0\perp c} \end{pmatrix}, \tag{4.5}$$

where

$$T_1 = b_0 + 2\sum_{j=1}^{\infty} b_j \cos(j\theta_c) \tag{4.6a}$$

$$T_2 = a_0 + 2\sum_{j=1}^{\infty} a_j \cos(j\theta_c), \tag{4.6b}$$

where the direction of propagation of the incident wave is along the positive x-direction in the cylinder coordinate system. The coefficients are given by (Bohren and Huffman, 1983):

$$a_j = \{[D_j(m_a\beta)/m_a + j/\beta]J_j(\beta) - J_{j-1}(\beta)]\}/ \{[D_j(m_a\beta)/m_a + j/\beta]H_j^{(1)}(\beta) - H_{j-1}^{(1)}(\beta)\}, \tag{4.7a}$$

$$b_j = \{[m_a D_j(m_a\beta) + j/\beta]J_j(\beta) - J_{j-1}(\beta)]\}/ \{[m_a D_j(m_a\beta) + j/\beta]H_j^{(1)}(\beta) - H_{j-1}^{(1)}(\beta)\}, \tag{4.7b}$$

where

$$D_j(\beta) = J_j'(\beta)/J_j(\beta). \tag{4.7c}$$

Here $J_j(x)$ is the Bessel function of the first kind of integral order j, and $J_j'(x)$ is the first derivative of $J_j(x)$ with respect to x. $H_j^{(1)}(x)$ is the Hankel function of the first kind, chosen such that the scattered wave is an outgoing wave for $\rho \to \infty$, and $\beta = k_0 a$, where a is the radius of the cylinder, as before. When the radius of the cylinder is sufficiently small that $\beta \ll 1$ and $m_a\beta \ll 1$, then the coefficients reduce considerably in complexity, so that

$$a_0 \approx i\pi\beta^4(m_a^2 - 1)/32, \quad b_0 \approx -i\pi\beta^2(m_a^2 - 1)/4,$$

$$a_1 \approx (-i\pi\beta^2/4)(m_a^2 - 1)/(m_a^2 + 1),$$

$$b_1 \approx -i\pi\beta^4(m_a^2 - 1)/32. \tag{4.8}$$

We have listed only these lowest order coefficients, since the higher order coefficients are higher order in β. To lowest order, up to and including β^2, the amplitude scattering elements become

$$T_1 \approx b_0, \qquad T_2 \approx -2a_1 \cos\theta_c. \tag{4.9}$$

In this lowest order, the scattered Poynting vectors, or the average power scattered per unit area, for incident polarizations parallel and perpendicular to the cylinder axis, in the Mie scattering method, are given by:

$$\begin{pmatrix} \mathbf{S}_{s,\parallel c} \\ \mathbf{S}_{s,\perp c} \end{pmatrix}_{\text{Mie}} = (\mathbf{e}_\rho/\rho) \begin{pmatrix} U_{\parallel c} \\ U_{\perp c}\cos^2\theta_c \end{pmatrix}, \tag{4.10}$$

where

$$\begin{pmatrix} U_{\parallel c} \\ U_{\perp c} \end{pmatrix} = I_0(2a)(\pi\beta^3/16)(m_a^2 - 1)^2 \begin{pmatrix} 1 \\ [4/(m_a^2 + 1)^2] \end{pmatrix}. \quad (4.11)$$

In the Shifrin method, as outlined in Sec. III, the scattered intensity has been found in spherical coordinates for a cylinder of finite length ℓ, and the reference polarizations were found with respect to the scattering plane, rather than to the cylinder axis. In order to compare these two methods, we will start with the Shifrin expressions, take the limit as ℓ approaches infinity, and convert to the cylindrical coordinates of the Mie method.

Since for long cylinders, $\phi_c \approx \phi - \pi/2$, for light polarized parallel to the cylinder axis, $\gamma = \phi_c \approx \phi - \pi/2$, while for light polarized perpendicular to the cylinder axis, $\gamma = \phi_c + \pi/2 \approx \phi$. Then for scattered light polarized initially either parallel or perpendicular to the cylinder axis, $\mathbf{e}_{ps,\text{Shifrin}}$, from Eq. 3.15 reduces to the forms

$$\mathbf{e}_{ps,\parallel c} = \mathbf{e}_{s\perp}, \qquad \mathbf{e}_{ps,\perp c} = -\mathbf{e}_{s\parallel}. \quad (4.13)$$

The scattered Poynting vectors for the two polarizations parallel and perpendicular to the cylinder axis in the Shifrin method then become

$$\begin{pmatrix} \mathbf{S}_{s,\parallel c} \\ \mathbf{S}_{s,\perp c} \end{pmatrix}_{\text{Shifrin}} = (\ell/2\pi)\beta\mathcal{L}f^2(\theta,\phi)(\mathbf{e}_r/r^2) \begin{pmatrix} U_{\parallel c} \\ U_{\perp c}\cos^2\theta \end{pmatrix}, \quad (4.14)$$

where $\mathcal{L} = \ell/a$, the ratio of the length to radius of the cylinder. We first convert to Cartesian coordinates, as shown in Fig. 1, with x_T along the length of the cylinder, and then make the replacement $x_T \rightarrow z_c$ and $z \rightarrow -x_c$ in order to convert to the coordinates of the cylinder. The relevant quantity in $f(\theta,\phi)$, given in Eq. 2.17 for thin rods at normal incidence, then assumes the form

$$(k_0\ell/2)\sin\theta\cos(\phi - \phi_c) = (\beta\mathcal{L}/2)(z_c/r) \quad (4.15a)$$

and the factor $\cos^2\theta$ in Eq. 4.14 becomes

$$\cos^2\theta = (\rho^2/r^2)\cos^2\theta_c, \quad (4.15b)$$

where

$$x_c = \rho\cos\theta_c; \quad y_c = \rho\sin\theta_c; \quad z_c = z_c; \quad r^2 = \rho^2 + z_c^2. \quad (4.15c)$$

In order to compare the result obtained from the Mie scattering method with that obtained by the Shifrin method, we compare the energy scattered into an area dA at a distance r from the sample, i.e., we compare $\mathbf{S}_{\text{Shifrin}} \cdot \mathbf{e}_r$ dA with $\mathbf{S}_{\text{Mie}} \cdot \mathbf{e}_\rho$ dA, where $dA = r^2\sin\theta d\theta d\phi = \rho\, d\theta_c\, dz_c$. If we assume thin cylinders, we can easily take the limit as $\mathcal{L} \rightarrow \infty$, so that

$$\begin{aligned} \lim_{\mathcal{L}\rightarrow\infty} \mathcal{L}f^2(\theta,\phi) &= \lim_{\mathcal{L}\rightarrow\infty} \{\sin^2[(\beta z_c/2r)\mathcal{L}]/[(\beta z_c/2r)^2\mathcal{L}]\} \\ &= \lim_{\mathcal{L}\rightarrow\infty} (2\{1 - \cos[(\beta z_c/r)\mathcal{L}]\}/[(\beta z_c/r)^2\mathcal{L}]) \\ &= 2\pi\delta(\beta z_c/r) = (2\pi r/\beta)\delta(z_c), \end{aligned} \quad (4.16)$$

where $\delta(z)$ is the Dirac delta function. Thus the limiting form for long rods of the energy scattered into an energy dA, as calculated by the Shifrin method, becomes

$$\lim_{\mathcal{L}\rightarrow\infty} \begin{pmatrix} \mathbf{S}_{s,\parallel c} \cdot \mathbf{e}_r \\ \mathbf{S}_{s,\perp c} \cdot \mathbf{e}_r \end{pmatrix}_{\text{Shifrin}} r^2\sin\theta d\theta d\phi = [\ell\delta(z_c)/\rho]\rho d\theta_c dz_c \begin{pmatrix} U_{\parallel c} \\ U_{\perp c}\cos^2\theta_c \end{pmatrix} \quad (4.17)$$

since $\delta(z_c)g(r) = \delta(z_c)g(\rho)$ for any function $g(r)$. This means that the Mie scattering result is actually the energy scattered per unit length of the cylinder, as seen in the plane $z = 0$. If we multiply Eq. 4.10 by the length ℓ and by the delta function $\delta(z_c)$, then we see that the lowest approximation for a thin cylinder at normal incidence, starting from the Mie scattering method, yields the same result as the Shifrin method, i.e.,

$$\begin{pmatrix} \mathbf{S}_{s,\parallel c} \cdot \mathbf{e}_p \\ \mathbf{S}_{s,\perp c} \cdot \mathbf{e}_p \end{pmatrix}_{\text{Mie}} \rho\, d\theta_c dz = [\ell\delta(z_c)/\rho]\rho\, d\theta_c dz_c \begin{pmatrix} U_{\parallel c} \\ U_{\perp c}\cos^2\theta_c \end{pmatrix}. \quad (4.18)$$

Therefore, we see that for long thin cylinders, the Shifrin method provides a solution that is as accurate as the Mie approach. For this reason, we will use the Shifrin method in Sec. V in calculations of light scattering from an array of HbS polymers.

V. APPLICATION TO SICKLE HEMOGLOBIN POLYMERS

In order to illustrate the advantage of the Shifrin method over the Rayleigh-Debye method, we now concentrate on sickle hemoglobin and propose two experimental configurations for a solution of sickle polymers for which our calculations are applicable. In both of these configurations, we assume that all the polymers are long thin cylindrical particles, as discussed in the previous sections, all of the same radius, and that the polymer concentration is sufficiently low that the distance between adjacent polymers is large compared with the wavelength of light. In both cases, we assume that the incident light strikes every polymer perpendicular to its axis. In the first configuration, shown in Fig. 2 *a*, all the polymers lie in

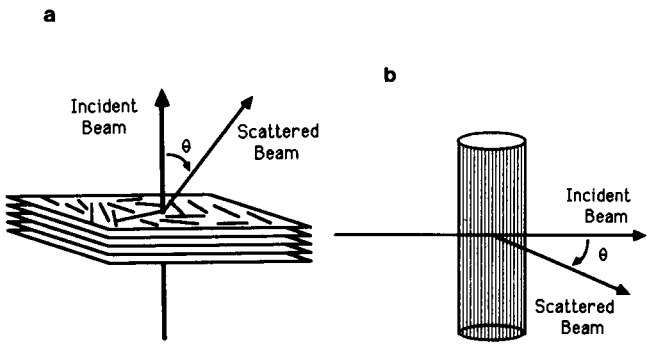

FIGURE 2 Models for light scattering in which (*a*) polymers lie in stratified planes, with the incident beam normal to the planes and (*b*) polymers are aligned within a capillary, with the incident beam perpendicular to the axis of the capillary.

striated planes, such that the incident light is perpendicular to all the planes and thus to the axes of all the cylindrical polymers. The polymers can either be oriented all in the same direction or oriented randomly within each plane. In the second configuration, we assume that all the polymers are aligned within a capillary tube, where the light is incident normally on the capillary tube and thus on the polymers, and we measure scattering at angles θ around the capillary, as shown in Fig. 2 *b*. This was the experimental setup used by Kam and Hofrichter (1986) in their study of inelastic light scattering from HbS polymers, although in that experiment the concentration of polymers was too high for our theory to be valid.

Before we present the results of calculations comparing the Shifrin and Rayleigh-Debye methods, we will calculate the theoretical limits of applicability for the Rayleigh-Debye method, as presented in Sec. II, i.e., $|m - 1| \ll 1$ and $k_0 d\,|m - 1| \ll 1$, where d is a characteristic linear dimension of the particle. As shown in the Appendix, for a concentration c = 40 g/dl, the ratio of the index of refraction of hemoglobin relative to its surrounding solution is $m_a \sim 1.13$, so that $|m_a - 1| = 0.13$, which is nearly out of the range of limitation of the first condition. The diameter of an Hb polymer is $d \sim 200$ Å (Dykes et al., 1979) so that for a wavelength $\lambda_0 = 5{,}145$ Å (Ferrone et al., 1985*a*), the quantity $k_0 d\,|m_a - 1|$ evaluated with this diameter yields a value of about 3×10^{-2}, which is well within the range of validity. However, for polymers that have aspect ratios of 20, L ~ 4,000 Å, which means that $k_0 L\,|m - 1| = 0.7$, definitely out of the valid range. For an aspect ratio of 100, the situation is even worse, since L ~ 20,000 Å and $k_0 L\,|m - 1| = 3$. We will show that for cylinders long compared to the wavelength of light, because of the breakdown of these conditions for the validity of the Rayleigh-Debye approach, the differences between the two methods can be significant, both qualitatively and quantitatively. By contrast, for aspect ratios of 20 or greater, the Shifrin model, as presented in Sec. III and applied to polymers long compared with the wavelength, works well.

In Fig. 3, we plot two orthogonal components of the intensity of scattered light versus polarization angle, calculated by the Shifrin method. The upper solid curve is the component of light scattering from aligned polymers polarized the same as Rayleigh-Debye scattering, calculated from Eq. 3.22 of Sec. III, and the lower solid curve, magnified by a factor of 100, is the rotated component, calculated from Eq. 3.23. The upper and lower dashed curves are the corresponding results for randomly oriented polymers within planes perpendicular to the incident beam, or, equivalently, for unpolarized incident light with any configuration of polymers within the planes, or for unpolarized light incident on aligned polymers within a capillary tube. These were calculated from Eqs. 3.24b and 3.24c. Results were normalized by the magnitude of Rayleigh-Debye scattering at $(\phi - \gamma) = 0°$, the angle at which the electric field is parallel to the aligned polymers. If the two methods produced identical results, the component of light scattering calculated by the Shifrin method that is polarized parallel to that of Rayleigh scattering should be unity for all polarization angles, and the rotated component should be zero. However, note that when the polymers are aligned, the Shifrin method gives a value of ~0.75 for the polarized component when the electric field is perpendicular to the cylinders. In addition, a small rotated component emerges. Even for random orientations within planes or

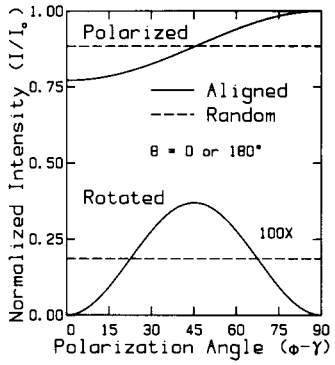

FIGURE 3 Polarization analyzed normal incidence light scattering calculated by the Shifrin method as a function of incident polarization angle, for the scattering angle θ of 0 or 180°, where the polymers are either aligned or randomly oriented. The upper curves show light scattering polarized the same as Rayleigh scattering, calculated from Eqs. 3.22 and 3.24b, and the lower curves the rotated component, polarized 90° with respect to Rayleigh scattering, calculated from Eqs. 3.23 and 3.24c. The lower curves have been magnified by a factor of 100. The curves are nomalized to unity for the polarization angle $(\phi - \gamma) = 90°$.

for unpolarized incident light, the magnitude of the parallel polarized component is reduced below that for Rayleigh-Debye scattering, and the rotated component is nonzero.

In Fig. 4, we plot the total intensity for scattering from aligned polymers as a function of scattering angle for both the Shifrin and Rayleigh-Debye methods, for several polarization angles. The solid curves were calculated with the Shifrin method, using Eq. 3.19 of Sec. III, and the dashed curves with the Rayleigh-Debye method using Eq. 2.18 of Sec. II. When the scattering angle is in the near forward or near backward directions, the difference between the two methods is the greatest i.e., almost 25%, with agreement occuring when the scattered light is perpendicular to the incident beam. In Fig. 5, we plot the same quantities for either polymers randomly oriented within their planes or for unpolarized light incident on aligned polymers. The solid curves were calculated with the Shifrin method using Eq. 3.24a of Sec. III, and the dashed curves were calculated with the Rayleigh-Debye method using Eq. 2.19 of Sec. II. Even for this case, for near forward or backward scattering, the difference is almost 15%.

In order to calculate magnitudes of scattered light, we note that if we multiply the expressions in Secs. II and III by r^2, we obtain the time averaged energy scattered into an infinitesimal solid angle $d\Omega$ in the direction of $\mathbf{e}_r$, i.e., at the scattering angles θ and ϕ. If this were integrated over the solid angle of aperture of the detector, then this would be the actual experimentally measured quantity. If we assume that the polymers are long compared with the wavelength of light, then the expression for $f(\theta, \phi)$ given by Eq. 2.17 peaks sharply at $(\phi - \phi_c) = 90°$, and we can use the limiting form given by Eq. 4.16. It is then most convenient to convert to cylindrical coordinates, as in Sec.

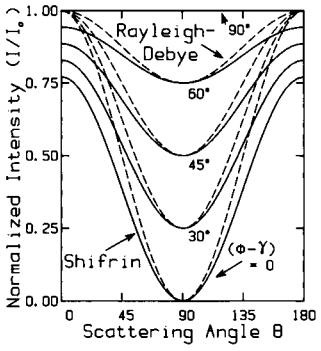

FIGURE 4 Light scattering from oriented polymers as a function of scattering angle θ for incident polarization angles $(\phi - \gamma)$ ranging from 0 to 90°. The dashed curves are obtained from the Rayleigh-Debye theory, calculated from Eq. 2.18 and the solid curves from the Shifrin theory, calculated from Eq. 3.19.

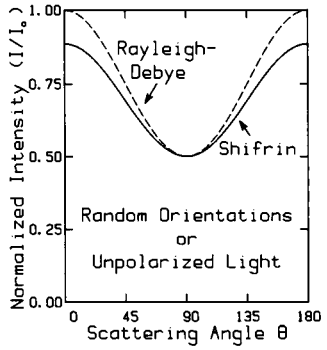

FIGURE 5 Light scattering incident with incident unpolarized light or random orientations of polymers for the Rayleigh-Debye method, calculated from Eq. 2.19 (*dashed curve*), and Shifrin method, calculated from Eq. 3.24a (*solid curve*), as a function of scattering angle θ.

IV, in order to obtain a more manageable expression for the relative scattering intensity given by the Shifrin method. We start with Eq. 3.19, multiply by the area $dA = \rho\ d\theta_c\ dz_c$ of the aperture of the detector and integrate over the delta function in z_c, which produces the result:

$$\iint \lim_{\mathcal{L}\to\infty} (I/I_0)\, dA = \int_{\text{aperture}} d\theta_c (k_0^3 a^2 V/8) \cdot (m_a^2 - 1)^2 T^2_{\text{pc,Shifrin}}, \quad (5.1a)$$

where

$$T^2_{\text{pc,Shifrin}} = \{(A_{\perp c}/A_{\parallel c})^2 \cos^2\theta_c \sin^2(\gamma - \phi_c) + \cos^2(\gamma - \phi_c)\}. \quad (5.1b)$$

This expression gives the power entering the aperture per unit incident intensity for scattering from a single polymer. Integrating Eq. 5.1a over all angles $\theta_c = 0$ to 2π produces an extinction cross section in agreement with van de Hulst (1981), p. 316.

In order to obtain the magnitude of scattering from a solution of polymers, we assume that, because the solution is dilute, the intensities simply add, so that we need merely multiply Eq. 5.1a by the total number of polymers in the scattering volume. This number is more conveniently expressed in terms of the volume fraction f of the solution occupied by hemoglobin molecules (free or bound in polymers), and the fraction η of hemoglobin that is bound in polymers. Using $f = c_0/c_{\max}$, where c_0 is the total Hb concentration and $c_{\max} = 127$ g/dl is the maximum concentration if the total volume were hemoglobin, as discussed in the Appendix, f and η can, in turn, be related to ζ, the fractional extent of the reaction, as

$$f\eta = \zeta(c_0 - c_s)/c_{\max}, \quad (5.2)$$

where $c_s = 19.26$ g/dl at 20.3°C is the solubility for the

solution (Ross et al., 1977) and ζ varies from 0 to 1 during the course of the reaction.

The number of polymers, multiplied by the volume V of a single polymer, and divided by the total scattering volume V_{sca}, is given by:

$$(NV/V_{sca}) = f\eta,$$

which is the fractional volume occupied by polymers. If the scattering volume is assumed to have a cylindrical shape of depth d, then the power P_{det} entering the detector, divided by the power P_{inc} of the incident beam, for oriented polymers, is then given by:

$$(P_{det}/P_{inc})_{oriented} = Wd \int_{aperture} d\theta_c T^2_{pc,Shifrin} \qquad (5.3a)$$

where

$$W = \zeta[(c_0 - c_s)/c_{max}](k_0^3 a^2/8)\,(m_a^2 - 1). \qquad (5.3b)$$

Using the numerical values $c_0 = 40$ g/dl and $m_a = 1.13$, as in the Appendix; $\lambda_0 = 5{,}145$ Å and d = 4 μm, as in Ferrone et al. (1985*a*); $a = 100$ Å, as determined by Dykes et al. (1979); and $\zeta = 0.1$, we find that $Wd = 7.9 \times 10^{-4}$. For a small aperture angle, one must simply multiply this number times $T_{pc,Shifrin}$, from Eq. 5.1b, evaluated at the angle θ_c of the detector relative to the oriented polymers and by the aperture angle in radians.

For unpolarized incident light, or for randomly oriented polymers, we average over γ or ϕ_c, yielding

$$(P_{det}/P_{inc})_{unpol} = \frac{Wd}{2} \int_{aperture} d\theta_c\{(A_{\perp c}/A_{\parallel c})^2 \cos^2\theta_c + 1\}. \qquad (5.4)$$

Integrating over all angles from 0 to 2π produces (P_{ext}/P_{inc}), the total fraction of power extinguished from the incident beam for oriented polymers, from Eq. 5.3, or for randomly oriented or unpolarized incident light, from Eq. 5.4:

$$(P_{ext}/P_{inc})_{oriented} = 2\pi Wd\{(1/2)(A_{\perp c}/A_{\parallel c})^2 \cdot \sin^2(\gamma - \phi_c) + \cos^2(\gamma - \phi_c)\} \qquad (5.5a)$$

$$(P_{ext}/P_{inc})_{unpol} = \pi Wd(\{(1/2)(A_{\perp c}/A_{\parallel c})^2 + 1\}. \qquad (5.5b)$$

If $A_{\perp c} = A_{\parallel c}$, we recover the results for the Rayleigh-Debye theory. Since $(A_{\perp c}/A_{\parallel c}) = 2/(m_a^2 + 1) = 0.88$, this means that, for oriented polymers, the extinction for the incident polarization $(\gamma - \phi_c) = 90°$ is smaller by a factor of 0.39 compared with the incident polarization $(\gamma - \phi_c) = 0$, while for Rayleigh-Debye theory, it would be smaller by a factor of 0.5. Thus, the Shifrin method produces quantitatively different results for the magnitude of the scattering and the extinction as does the Rayleigh-Debye theory.

VI. CONCLUSIONS

We have shown that for sickle hemoglobin polymers long compared with the wavelength of light, the Rayleigh-Debye method for calculating light scattering as a function of incident polarization and scattering angle can produce large qualitative and quantitative errors (as much as 25%) and that the Shifrin method can provide accurate results. These effects should be observable experimentally, since the shapes of the light scattering curves, and not only their overall magnitudes, are different in the two cases. The errors are largest when the polymers are aligned but are still significant (15%) when the polymers are randomly oriented. Not only is the angular dependence of the scattering in error, but the extinction (turbidity) as well. The use of the Shifrin method is thus essential in explaining experimental results.

We have shown that for the special case of long rigid polymers, the Shifrin method works as well as the exact (Mie) approach. In addition, the Shifrin method is not limited by all the approximations we have made in this paper; unlike the Mie approximation, it can easily be extended to scattering at any angle of incidence and can be used for various shapes of particles. The method has the most difficulty when one of the dimensions of the particle is close to the wavelength of light. However, this paper illustrates that the Rayleigh-Debye method, which is used in many applications, is not valid even for a simple system of dilute rigid polymers. It should certainly not be extended to more complicated geometries.

The results presented here for sickle hemoglobin are valid in the regime in which the polymers are well separated compared with the wavelength of light, either at the beginning of a polymerization reaction (Ferrone et al., 1985*a*, *b*), or for polymerization occurring in high phosphate solutions (Adachi and Asakura, 1978, 1979*a*, 1983). Experiments for concentrated solutions of hemoglobin (Ferrone et al., 1987; Basak et al., 1988), suggest that polymers form first in disordered arrays, and undergo an alignment transition. Whether or not polymers align during growth in high phosphate solutions would provide further insight into the formation of highly ordered domains.

The numerical calculations here were done for incident light in a region where the absorption is low. The effects of absorption can easily be included through the use of the complex dielectric constant or index of refraction, where the imaginary part of the index of refraction is directly proportional to the absorption. Unfortunately, the only data available for the index of refraction inside a sickle hemoglobin polymer had to be extracted from measurements of a solution of hemoglobin using a broad band red

spectrum (Rossi-Fanelli et al., 1961; Jones et al., 1978), as shown in the Appendix. In order for the calculations presented in this paper to incorporate properly the anisotropy in both the real and imaginary (absorption) parts of the index of refraction, measurements of index of refraction as a function of orientation need to be done on single crystals of deoxyhemoglobin, as a function of wavelength throughout the visible range.

Further theoretical work on light scattering in dilute solutions of sickle hemoglobin polymers is in progress. This includes extensions of the present work to different lengths of polymers and to incident light at an arbitrary angle relative to the polymers. Other work is concerned with the changes in the effective dielectric constant of a hemoglobin solution due to the presence of polymers, which for higher concentrations must be included in the estimated value for the dielectric constant surrounding a polymer that scatters light.

APPENDIX

Dielectric constant for hemoglobin

Although the dielectric constant ϵ_H inside a sickle hemoglobin polymer in the optical spectrum has not been measured, its value can be extracted from data for the index of refraction n_m of a solution of hemoglobin monomers. This quantity was measured as a function of concentration c of hemoglobin using a broad spectrum of red light, with the result (Rossi-Fanelli et al., 1961; Jones et al., 1978):

$$n_m = n_w + \beta c, \tag{A.1}$$

where $n_w = 1.334$ is the index of refraction of water and $\beta = 0.00197$ with c in g/dl. A solution of hemoglobin can be considered to be a composite medium consisting of hemoglobin particles and water particles. Given the dielectric constants inside both types of particles, effective medium theories predict the effective dielectric constant of the medium, or the dielectric constant of a uniform medium that would have the same optical properties as the composite medium. In our case, the dielectric constant, $\epsilon_w = n_w^2$, of water is known, and so is the effective dielectric constant of the composite medium i.e., $\epsilon_m = n_m^2$. The unknown is thus the dielectric constant ϵ_H of hemoglobin, which can be obtained from the theory for the effective medium. In order to accomplish this in practice, we employ Bruggeman's symmetrical effective medium approximation (Bruggeman, 1935; Landauer, 1978). This is superior to the Maxwell-Garnett approximation because it is applicable to high concentrations of hemoglobin (i.e., large volume fractions), whereas the Maxwell-Garnett approximation would only be valid for low concentrations (small volume fractions) (Maxwell-Garnett, 1904; Landauer, 1978).

This approximation requires that the dipole moments of all the particles comprising the effective medium, in which each particle is assumed to be embedded in the effective medium, must sum to zero. Suppose we consider a solution of hemoglobin monomers to be composed of spherical hemoglobin particles of dielectric constant ϵ_H and of spherical water particles of dielectric constant ϵ_W. Suppose further that the hemoglobin occupies a fraction f of the solution, and the water a fraction $(1 - f)$. Then, if c is the concentration of the solution, and c_{max} is the maximum concentration if the solution were totally hemoglobin, then $f = c/c_{max}$. If $\mathbf{p}_H$ is the dipole moment of a hemoglobin molecule embedded in the effective medium, then

$$\mathbf{p}_H = (3/4\pi)V(\epsilon_H - \epsilon_m)/(\epsilon_H + 2\epsilon_m)\,\mathbf{E}_0, \tag{A.2}$$

where V is the volume of the molecule and $\mathbf{E}_0$ is the electric field far from the molecule. A water particle embedded in the same effective medium would have an analogous dipole moment, $\mathbf{p}_W$, which can be obtained from Eq. A.2 by replacing all H subscripts by W, assuming that a water particle has the same volume as a hemoglobin particle. If $\mathbf{E}_0$ is then the average field in the effective medium i.e.,

$$\mathbf{E}_0 = \epsilon_m \mathbf{E}_{ext}, \tag{A.3}$$

where $\mathbf{E}_{ext}$ is the externally applied electric field, then all deviations from this must average to zero. This means that the dipole moments of all particles embedded in the effective medium must add to zero i.e.,

$$f\mathbf{p}_H + (1 - f)\mathbf{p}_W = 0, \tag{A.4}$$

or, simplifying and writing in terms of ϵ_W, ϵ_H, and ϵ_m,

$$f(\epsilon_H - \epsilon_m)/(\epsilon_H + 2\epsilon_m) + (1 - f)(\epsilon_W - \epsilon_m)/(\epsilon_W + 2\epsilon_m) = 0. \tag{A.5}$$

The known quantities in Eq. A.5 are f, $\epsilon_m = n_m^2$, and ϵ_W. This equation then allows us to determine the dielectric constant ϵ_H inside a hemoglobin molecule. In order to extract this value, we first solve for ϵ_m to first order in f, for the case that the concentration of hemoglobin is low, with the result:

$$\epsilon_m \approx \epsilon_W + [3\epsilon_W(\epsilon_H - \epsilon_W)/(\epsilon_H + 2\epsilon_W)]f. \tag{A.6}$$

If we square Eq. A.1 and make the same approximation, we obtain a similar form:

$$\epsilon_m \approx \epsilon_W + [2\beta c_{max}\epsilon_W]f. \tag{A.7}$$

If we now equate coefficients of f in Eqs. A.6 and A.7, we obtain the following expression for ϵ_H:

$$\epsilon_H \approx \epsilon_W\{[1 + (4/3)\beta c_{max}/n_W]/[1 - (2/3)\beta c_{max}/n_W]\}, \tag{A.8}$$

where, as before, $\epsilon_W = n_m^2$.

In order to evaluate Eq. A.8, we require a value for c_{max}, the maximum concentration of hemoglobin, which can be obtained from the specific volume, $V = 0.79$ cm^3/g. This value has been determined by fitting the monomer activity coefficient with a theoretical expression for the activity coefficient for monomers in powers of the concentration (Ferrone et al., 1985*b*; Minton, 1983; Ross and Minton, 1977; Ross et al., 1978; Sunshine et al., 1982). In this case, $c_{max} = (1/V) = 127$ g/dl, which yields a value of $\epsilon_H \approx 2.54$.

In order to study light scattering for a polymer immersed in a solution of hemoglobin, we actually require the ratio of the dielectric constant of hemoglobin to that of the solution i.e., ϵ_H/ϵ_m. The results of calculating ϵ_m from Eq. A.5, with $\epsilon_H = 2.54$ appear in Fig. 6. For $c = 40$ g/dl, $\epsilon_m = 2.00$, so that $\epsilon_H/\epsilon_m = 1.27$ or $n_H/n_m = m_a = 1.13$. This is the value that has been used in the light scattering calculations of Sec. V.

The calculations that we present here were performed with the assumption that the effects of absorption can be neglected, so that the dielectric constant and index of refraction have been assumed to be real. In the presence of absorption, since the index of refraction is complex, $n = n_R + in_I$, with the absorption coefficient γ directly proportional to n_I i.e., $\gamma = 4\pi n_I/\lambda$, where λ is the wavelength (van de Hulst, 1981, p. 267). Using values for the absorption coefficients of hemoglobin crystals (Eaton and Hofrichter, 1978), we find that for $\lambda = 5{,}145$ Å, $\gamma = 250$ cm^{-1} and $n_I \approx 10^{-3}$ and for $\lambda = 4{,}300$ Å (the peak of the Soret band),

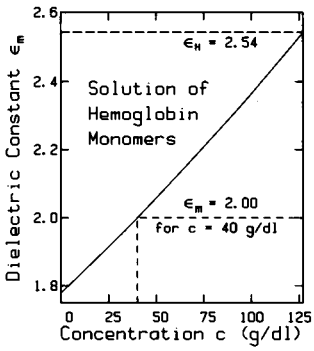

FIGURE 6 Dielectric constant ϵ_m for a solution of hemoglobin monomers as a function of concentration. On the graph are shown the values obtained for the dielectric constant, $\epsilon_H = 2.54$, inside a hemoglobin monomer and for the effective dielectric constant of the solution $\epsilon_m = 2.00$, for a concentration c = 40 g/dl.

$\gamma = 10^4\ cm^{-1}$ (for E ∥ c* axis) and $n_I \approx 0.03$. For $\lambda = 5{,}145$ Å, n_I is small compared with $n_R = 1.59$, so that it can be neglected. However, at the peak of the Soret band, n_I is sufficiently large that it should be included. This extension will be considered in future work.

The author would like to thank Dr. Frank A. Ferrone for encouragement and enlightening conversations throughout the course of this work, and would additionally like to acknowledge Alice Presley, Dr. L. D. Cohen, and Dr. R. D. Haracz for helpful discussions.

This work was supported by the National Institutes of Health through grant HL38614.

Received for publication 28 February 1989 and in final form 12 June 1989.

REFERENCES

Acquista, Charles. 1976. Light scattering by tenuous particles: a generalization of the Rayleigh-Gans-Rocard approach. *Appl. Opt.* 15:2932–2936.

Acquista, Charles. 1980. Shifrin's method applied to scattering by tenuous non-spherical particles. *In* Light Scattering By Irregularly-Shaped Particles. Plenum Publishing Corp., New York. Donald W. Schauerman, editor. 165–168.

Adachi, K., and T. Asakura. 1978. Demonstration of a delay time during aggregation of diluted solutions of deoxyhemoglobin S and hemoglobin C_{Harlem} in concentrated phosphate buffer. *J. Biol. Chem.* 253:6641–6643.

Adachi, K., and T. Asakura. 1979. Nucleation-controlled aggregation of deoxyhemoglobin S: possible difference in the size of nuclei in different phosphate concentrations. *J. Biol. Chem.* 254:7765–777.

Adachi, K., and T. Asakura. 1982. Kinetics of the polymerization of hemoglobin in high and low phosphate buffers. *Blood Cells (Berl.).* 8:213–224.

Adachi, K., and T. Asakura. 1983. Multiple nature of polymers of deoxyhemoglobin S prepared by different methods. *J. Biol. Chem.* 258:3045–3050.

Amos, L. A. 1982. Tubulin and associated proteins. *In* Electron microscopy of proteins. Vol. 3. J. R. Harris, editor. Academic Press Inc., New York. 207–250.

Andreo, R. H., and R. A. Farrell. 1982. Corneal small-angle light-scattering theory: wavy fibril models. *J. Opt. Soc. Am.* 72:1479–1492.

Basak, S., F. A. Ferrone, and J. T. Wang. 1988. The kinetics of domain formation by sickle hemoglobin polymers. *Biophys. J.* 54:829–843.

Benedek, G. B. 1971. Theory of transparency of the eye. *Appl. Opt.* 10:459–473.

Berne, B. J. 1974. Appendix: interpretation of the light scattering from long rods. *J. Mol. Biol.* 89:755–758.

Berne, B. J., and R. Pecora. 1976. Dynamic Light Scattering with Applications to Chemistry, Biology, and Physics. John Wiley & Sons, New York. 376 pp.

Bohren, C. F., and D. R. Huffman. 1983. Absorption and Scattering of Light by Small Particles. John Wiley & Sons, New York. 530 pp.

Briehl, R. W., and G. W. Christoph. 1987. Exponential progress curves and shear in the gelation of hemoglobin S. *Prog. Clin. Biol. Res.* 240:129–149.

Bruggeman, D. A. G. 1935. Berechnung verschiedener physikalischer konstanten von heterogenen substanzen. I. Dielektrizitätskonstanten und leitfähigkeiten der mischkörper aus isotropen substanzen. *Ann. Phys. (Leipz.).* 24:636–664.

Burchard, W. 1983. Static and dynamic light scattering from branched polymers and biopolymers. *Adv. Polym. Sci.* 48:1–124.

Camerini-Otero, R. D., and L. A. Day. 1978. The wavelength dependence of the turbidity of solutions of macromolecules. *Biopolymers.* 17:2241–2249.

Casassa, E. F. 1955. Light scattering from very long rod-like particles and an application to polymerized fibrinogen. *J. Chem. Phys.* 23:596–597.

Christoph, G. W., and R. W. Briehl. 1983. Exponential progress curves in the gelation of deoxyhemoglobin S. *Biophys. J.* 41:415a. (Abstr.)

Cohen, A. S., T. Shirahama, and M. Skinner. 1982. Electron microscopy of amyloid. *Electron Microsc. Proteins.* 3:165–205.

Cohen, L. D., R. D. Haracz, A. Cohen, and C. Acquista. 1983. Scattering of light from arbitrarily oriented finite cylinders. *Appl. Opt.* 22:742–748.

Cox, J. L., R. A. Farrell, R. W. Hart, and M. E. Langham. 1970. The transparency of the mammalian cornea. *J. Physiol. (Lond.).* 210:601–616.

Craig, R., and P. Knight. 1982. Myosin molecules, thick filaments and the actin-myosin complex. *Electron Microsc. Proteins.* 4:97–203.

Debye, P. 1947. Molecular-weight determination by light scattering. *J. Phys. Chem.* 51:18–32.

Debye, P., and A. M. Bueche. 1950. Light scattering by concentrated polymer solutions. *J. Chem. Phys.* 18:1423–1425.

Delaye, M., and A. Tardieu. 1983. Short-range order of crystallin proteins accounts for eye lens transparency. *Nature (Lond.).* 302:415–417.

Dykes, G. W., R. H. Crepeau, and S. J. Edelstein. 1979. Three-dimensional reconstruction of the 14-filament fibers of hemoglobin S. *J. Mol. Biol.* 130:451–472.

Eaton, W. A., and J. Hofrichter. 1978. Polarized absorption and linear dichroism spectroscopy of hemoglobin. *Methods Enzymol.* 76:175–261.

Eaton, W. A., and J. Hofrichter. 1987. Hemoglobin S gelation and sickle cell disease. *Blood.* 70:1245–1266.

Elbaum, D., J. P. Harrington, R. M. Bookchin, and R. L. Nagel. 1978. Kinetics of HbS gelation: effect of alkylureas, ionic strength and other hemoglobins. *Biochim. Biophys. Acta.* 534:228–238.

Farrell, R. A., and R. L. McCally. 1976. On the interpretation of depth

dependent light scattering measurements in normal corneas. *Acta Ophthalmol.* 54:261–270.

Ferrone, F. A., J. Hofrichter, H. R. Sunshine, and W. A. Eaton. 1980. Kinetic studies on photolysis-induced gelation of sickle cell hemoglobin suggest a new mechanism. *Biophys. J.* 32:361–380.

Ferrone, F. A., J. Hofrichter, and W. A. Eaton. 1985*a*. Kinetics of sickle hemoglobin polymerization. I. Studies using temperature-jump and laser photolysis techniques. *J. Mol. Biol.* 183:591–610.

Ferrone, F. A., J. Hofrichter, and W. A. Eaton. 1985b. Kinetics of sickle hemoglobin polymerization. II. A double nucleation mechanism. *J. Mol. Biol.* 183:611–631.

Ferrone, F. A., M. R. Cho, and M. F. Bishop. 1986. Can a successful mechanism for HbS gelation predict sickle cell crises? *INSERM (Inst. Natl. Sante Rech. Med.) Colloq.* 141:53–66.

Ferrone, F. A., S. Basak, A. J. Martino, and H. X. Zhou. 1987. Polymer domains, gelation models and sickle cell crises. *Prog. Clin. Biol. Res.* 240:47–58.

Gaskin, F., C. R. Cantor, and M. L. Shelanski. 1974. Turbidimetric studies of the in Vitro assembly and disassembly of porcine neurotubules. *J. Mol. Biol.* 89:737–755.

Goldman, J. N., and G. B. Benedek. 1967. The relationship between morphology and transparency in the nonswelling corneal stroma of the shark. *Invest. Optomol.* 6:574–600.

Hantgan, R. R., and J. Hermans. 1979. Assembly of fibrin: a light scattering study. *J. Biol. Chem.* 254:11272–1128.

Hart, R. W., and R. A. Farrell. 1969. Light scattering in the cornea. *J. Opt. Soc. Am.* 59:766–774.

Hofrichter, J., J. S. Gethner, and W. A. Eaton. 1978. Mechanism of sickle cell hemoglobin gelation. *Biophys. J.* 24:20a. (Abstr.)

Hofrichter, J. 1986. Kinetics of sickle hemoglobin polymerization. III. Nucleation rates determined from stochastic fluctuations in polymerization progress curves. *J. Mol. Biol.* 189:553–571.

Jones, C. R., C. S. Johnson, Jr., and J. T. Penniston. 1978. Correlation spectroscopy of hemoglobin: diffusion of oxy-HbA and oxy-HbS. *Biopolymers.* 17:1581–1593.

Kam, Z., and J. Hofrichter. 1986. Quasi-elastic laser light scattering from solutions and gels of hemoglobin S. *Biophys. J.* 50:1015–1020.

Kerker, M. 1969. The Scattering of Light and other Electromagnetic Radiation. Academic Press Inc., New York.

Kratochvil, P. 1972. Particle scattering functions. *In* Light Scattering from Polymer Solutions. M. B. Huglin, editor. Academic Press Inc., New York. 333–384.

Landau, L. D., and E. M. Lifshitz. 1960. Electrodynamics of Continuous Media. Addison-Wesley Publishing Company, Reading, MA. 299–304.

Landauer, R. 1978. Electrical conductivity in inhomogeneous media. *Am. Inst. Phys. Conf. Proc.* 40:2–45.

Madonia, F., P. L. San Biagio, M. U. Palma, G. Schiliro, S. Musumeci, and G. Russo. 1983. Photon scattering as a probe of microviscosity and channel size in gels such as sickle haemoglobin. *Nature (Lond.).* 302:412–415.

Maurice, D. M. 1957. The structure and transparency of the cornea. *J. Physiol. (Lond.).* 136:263–286.

Maurice, D. M. 1962. The cornea and sclera. Academic Press Inc., New York. H. Davson, editor. *In* The Eye. 289–368.

Maxwell-Garnett, J. C. 1904. Colours in metal glasses and in metallic films. *Phil. Trans. Roy. Soc. Lond.* 203:385–419.

McCally, R. L., and R. A. Farrell. 1976. The depth dependence of light scattering from the normal rabbit cornea. *Exp. Eye Res.* 23:69–81.

Minton, A. P. 1983. The effect of volume occupancy upon the thermodynamic activity of proteins: some biochemical consequences. *Mol. Cell. Biochem.* 55:119–140.

Mitchison, T., and M. Kirschner. 1984*a*. Microtubule assembly nucleated by isolated centrosomes. *Nature (Lond.).* 312:232–237.

Mitchison, T., and M. Kirschner. 1984*b*. Dynamic instability of microtubule growth. *Nature (Lond.).* 312:237–242.

O'Brien, E. J., and M. J. Dickens. 1983. Actin and thin filaments. *In* Electron Microscopy of Proteins. Vol. 4. J. R. Harris, editor. Academic Press Inc., New York. 1–95.

Pumphrey, J. C., and J. Steinhardt. 1976. Formation of needle-like aggregates in stirred solutions of hemoglobin S. *Biochem. Biophys. Res. Commun.* 69:99–105.

Purich, D. L., and D. Kristofferson. 1984. Microtubule assembly: a review of progress, principles, and perspectives. *Adv. Protein Chem.* 36:133–212.

Ross, P. D., R. W. Briehl, and A. P. Minton. 1978. Temperature dependence of nonideality in concentrated solutions of hemoglobin. *Biopolymers.* 17:2285–2288.

Ross, P. D., J. Hofrichter, and W. A. Eaton. 1977. Themodynamics of gelation of sickle cell deoxyhemoglobin. *J. Mol. Biol.* 115:111–134.

Ross, P. D., and A. P. Minton. 1977. Analysis of non-ideal behavior in concentrated hemoglobin solutions. *J. Mol. Biol.* 112:437–452.

Rossi-Fanelli, A., E. Antonini, and A. Caputo. 1961. Studies on the relations between molecular and functional properties of hemoglobin. I. The effect of salts on the molecular weight of human hemoglobin. *J. Biol. Chem.* 236:391–396.

Serafini-Fracassini, A. 1982. The electron microscopy of fibrous proteins of connective tissue. *In* Electron Microscopy of Proteins. Vol. 2. J. R. Harris, editor. Academic Press Inc., New York. 195–231.

Shifrin, K. S. 1951. Scattering of light in a turbid medium. Moscow, 1951. (English translation: NASA TTF-477, Washington, D.C., 1968). 212 pp.

Steinert, P. M. 1981. Intermediate filaments. *In* Electron Microscopy of Proteins. Vol. 1. J. R. Harris, editor. Academic Press Inc., New York. 125–166.

Steinert, P. M., W. W. Idler, and S. B. Zimmerman. 1976. Self-assembly of bovine epidermal keratin filaments in vitro. *J. Mol. Biol.* 108:547–567.

Sunshine, H. R., J. Hofrichter, F. A. Ferrone, and W. A. Eaton. 1982. Oxygen binding by sickle cell hemoglobin polymers. *J. Mol. Biol.* 158:251–273.

Tanford, C. 1961. Physical chemistry of macromolecules. John Wiley & Sons Inc., New York. 710 pp.

Traub, W., and K. A. Piez. 1971. The chemistry and structure of collagen. *Adv. Protein Chem.* 25:243–352.

Van de Hulst, H. C. 1981. Light scattering by small particles. Dover Publications Inc., New York. 470 pp.

Wegner, A. 1982. Spontaneous fragmentation of actin filaments in physiological conditions. *Nature (Lond.).* 296:266–267.

Wegner, A. and P. Savko. 1982. Fragmentation of actin filaments. *Biochemistry.* 21:1909–1913.

Zimm, B. H., R. S. Stein, and P. Doty. 1945. Classical theory of light scattering from solutions—a review. *Polymer Bull.* 6:90–119.

Zimm, B. H. 1948. The Scattering of light and the radial distribution function of high polymer solutions. *J. Chem. Phys.* 16:1093–1099.

Zimm, B. H., and W. B. Dandliker. 1954. Theory of light scattering and refractive index of solutions of large colloidal particles. *J. Phys. Chem.* 58:644–648.